

# Lawrence Berkeley National Laboratory

## Recent Work

### Title

Designed asymmetric coordination helicates with bis- $\beta$ -diketonate ligands.

### Permalink

<https://escholarship.org/uc/item/7443g45j>

### Journal

Dalton transactions (Cambridge, England : 2003), 48(45)

### ISSN

1477-9226

### Authors

Diego, Rosa  
Darawsheh, Mohanad  
Barrios, Leoní A  
et al.

### Publication Date

2019-12-01

### DOI

10.1039/c9dt03398j

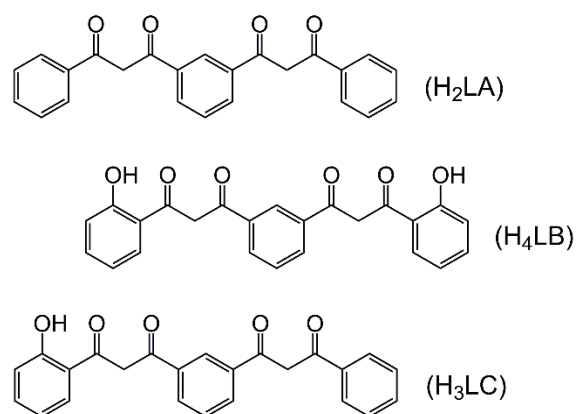
Peer reviewed

## Designed asymmetric coordination helicates with bis- $\beta$ -diketonate ligands.

Rosa Diego, Mohanad Darawsheh, Leoní A. Barrios, Anna Sadurní, Jordi García, Paul Lloyd-Williams, Simon J. Teat, Olivier Roubeau, David Aguilà and Guillem Aromí ORCID I

A new bis-( $\beta$ -diketone) ligand featuring built-up structural asymmetry yields the non-symmetric Fe(III) and Ga(III) dinuclear, triple-stranded helicates by design. Their structural properties have been studied, both in solid state and solution, and compared with their corresponding symmetric analogues. The robustness observed show the potential of this synthetic strategy to develop non-symmetric helicoidal motifs with specific functional groups.

Of the extensive range of structures derived from coordination supramolecular chemistry, metalohelicates have recently become highly topical due to the emergence of many potential applications. These helicoidal molecular architectures, based on two (or more) strand ligands wrapping one (or more) metal ion(s),<sup>1-3</sup> are studied, for example, as potential cancer treatment agents,<sup>4</sup> as molecular hardware for spin-based quantum computing,<sup>5</sup> in chirality switching applications<sup>6</sup> or as light-converting devices.<sup>7</sup> Among the different strategies to produce such supramolecular motifs, the use of bis-( $\beta$ -diketone) ligands has become an excellent approach due to their enormous synthetic versatility.<sup>8, 9</sup> One can, for example, functionalize  $\beta$ -diketonate helicates to tailor their interaction with specific biomolecular targets,<sup>10</sup> add electroactive units<sup>11</sup> or engineer the spacer of the ligand to allow photoswitchability.<sup>12</sup> Despite of such a potential, to date, only symmetric bis-( $\beta$ -diketonate) helicates have been reported, while the only non-symmetric bis-( $\beta$ -diketone) molecules found in the literature have been used as starting materials for a series of pyrazolyl-based ligands.<sup>13</sup> Taking into account that asymmetry in helicates is crucial for some specific tasks, such as the site selective disposition of metal ions within heterometallic compounds<sup>14, 15</sup> or the promotion of amphipathic character in the molecular system,<sup>4</sup> we decided to establish a new ligand-based strategy to produce asymmetric metalohelicates using diketonate units. For that, we first focused our attention on two symmetric bis-( $\beta$ -diketone) ligands, H<sub>2</sub>LA and H<sub>4</sub>LB (Scheme 1), that have been previously used by some of us to design symmetric helicates,<sup>16</sup> pairs of clusters<sup>17</sup> or linear metallic chains.<sup>18, 19</sup>



Scheme 1. Ligands H<sub>2</sub>LA, H<sub>4</sub>LB and H<sub>3</sub>LC.

Both ligands exhibit a central *meta*-phenylene spacer attached to two  $\beta$ -diketone units, capped at both ends with additional phenyl (H<sub>2</sub>LA) or hydroxyphenyl (H<sub>4</sub>LB) substituents. For this study, the potential of H<sub>4</sub>LB to promote likewise helicoidal topologies had not yet been explored. We have now ascertained this by making react three equivalents of the ligand with two equivalents of Fe(III) or Ga(III) in THF under moderate basic conditions (see Experimental Section, SI). Slow diffusion of diethyl ether into the resulting solutions afforded needle-shaped crystals of [Fe<sub>2</sub>(H<sub>2</sub>LB)<sub>3</sub>] (**1**) or block-shaped crystals of [Ga<sub>2</sub>(H<sub>2</sub>LB)<sub>3</sub>] (**2**), respectively. Single-crystal X-ray diffraction (SCXRD) was used to determine the molecular structure of both systems, confirming their helical topologies (Fig. 1, top, and Fig. S1).

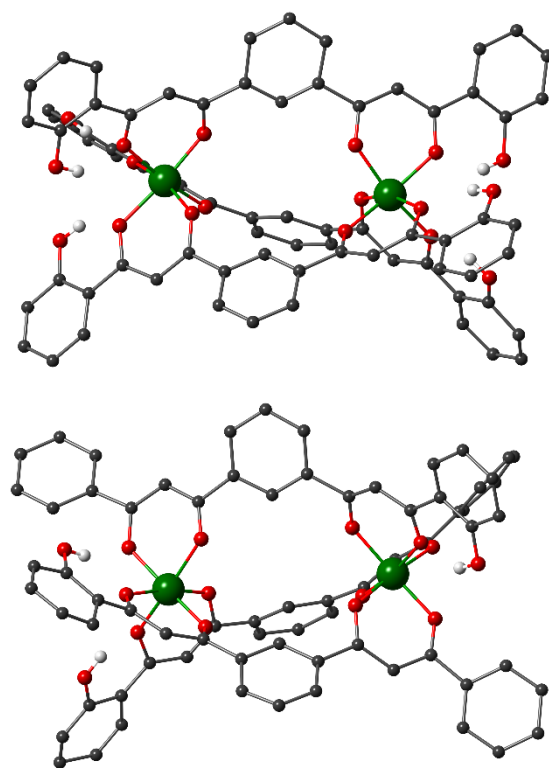


Figure 1. Representation of the molecular structure of [Fe<sub>2</sub>(H<sub>2</sub>LB)<sub>3</sub>] (top) and [Fe<sub>2</sub>(HLC)<sub>3</sub>] (bottom). For the former, only one crystallographically independent helicate is shown.

Complexes **1** and **2** crystallize in the  $P2_1/n$  and  $C2/c$  space groups, respectively, featuring both, right-handed ( $\Delta\Delta$ ) and left-handed ( $\Lambda\Lambda$ ) configurations in the unit cell (Table S1). The asymmetric unit of **1** exhibits three crystallographically independent molecules (Fig. S2) while only one is found for compound **2**. The crystal lattice of both compounds is filled with molecules of THF, as well as Et<sub>2</sub>O molecules for **1**. As observed for H<sub>2</sub>LA in the reported [M<sub>2</sub>(LA)<sub>3</sub>] metallohelicates (M=Ti, V, Mn, Fe),<sup>16</sup> the helicates here exhibit three H<sub>2</sub>LB<sup>2-</sup> ligands wrapping two Fe(III) or Ga(III) ions though their  $\beta$ -diketonate units, keeping them in average 7.16 and 7.23 Å apart, respectively (Tables S2 and S3). The resulting octahedral environment around each metal site was quantified by means of continuous-shape measures (CShMs,<sup>20</sup> Table S4). Similar results were obtained when assessing the crystal structure of [Fe<sub>2</sub>(LA)<sub>3</sub>], showing that both ligands have akin binding properties (Table S4). The potential of the two ligands to promote helicoidal species was further analyzed by characterizing the pitch  $L$  in [Fe<sub>2</sub>(LA)<sub>3</sub>] and [Fe<sub>2</sub>(H<sub>2</sub>LB)<sub>3</sub>], a parameter that measures the rate of the helical progression of the molecular strand as one advances along the axis of the helicate:

$$L = d / \left( \frac{\omega_1}{360} \right)$$

Here,  $d$  is the distance (Å) between two points of the helical axis, and  $\omega_1$  the angle twisted (°) in going from one point to the other.<sup>21</sup> This allows quantifying the helicoidal arrangement in each compound, and thus to evaluate the torsion experienced by the ligands in accommodating the octahedral twist at the Fe(III) centers. A total pitch,  $L_T$ , was defined by considering the distance between the centroids of the two most external triangular faces of the octahedral polyhedra of the metal ions (Fig. S3). The corresponding twist angle  $\omega_{1T}$ , was defined as the average of the torsion angles O-Fe1-Fe2-O of each strand (involving the outer oxygen donors of the two  $\beta$ -diketonate units). In addition, two local pitches,  $L_{Fe1}$  and  $L_{Fe2}$ , referred to the twist inside the polyhedra around Fe1 and Fe2, respectively, were also defined. For these,  $d$  is the distance between the centroids of the outer and the inner triangular faces of each octahedron, while  $\omega_1$  is the average of the three angles between both Fe-O vectors of each chelate, after projecting them on the plane perpendicular to the helical axis (Fig. S3). As expected, the values obtained for [Fe<sub>2</sub>(LA)<sub>3</sub>] and [Fe<sub>2</sub>(H<sub>2</sub>LB)<sub>3</sub>] were found to be similar, confirming the comparable twisting

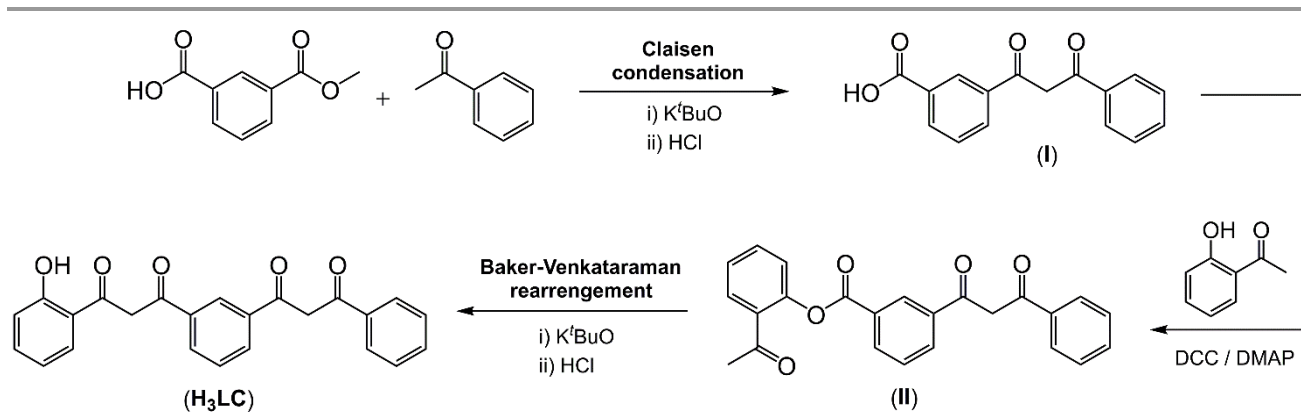
capabilities of the two corresponding symmetric ligands (Table 1). The slightly larger  $d$  values and smaller  $\omega_1$  angles observed in compound **1** evidence, nevertheless, the influence of the -OH groups from H<sub>2</sub>LB<sup>2-</sup>, which impose slightly larger pitch values. The stability of [Fe<sub>2</sub>(H<sub>2</sub>LB)<sub>3</sub>] in solution was confirmed by electrospray ionization mass spectrometry (ESI- MS) in CHCl<sub>3</sub>, which revealed the expected isotopic distribution (Fig. S4). This is in line with <sup>1</sup>H NMR experiments with the diamagnetic compound **2**, which demonstrates the integrity and high symmetry of the supramolecular structure (see below, Fig. 2, top).

**Table 1.** Linear distances ( $d$ ) and average twist angles ( $\omega_1$ ) defining the total ( $L_T$ ) and local ( $L_{Fe1}$  and  $L_{Fe2}$ ) helical pitches in compounds [Fe<sub>2</sub>(LA)<sub>3</sub>], [Fe<sub>2</sub>(H<sub>2</sub>LB)<sub>3</sub>] and [Fe<sub>2</sub>(HLC)<sub>3</sub>].

	[Fe <sub>2</sub> (LA) <sub>3</sub> ]	[Fe <sub>2</sub> (H <sub>2</sub> LB) <sub>3</sub> ] <sup>a</sup>	[Fe <sub>2</sub> (HLC) <sub>3</sub> ]
$d_{Fe1}$ (Å)	2.34	2.35 · 2.39 · 2.37	2.37
$\omega_{1(Fe1)}$ (°)	50.0	47.6 · 45.7 · 45.6	47.6
$L_{Fe1}$ (Å)	16.8	17.8 · 18.8 · 18.7	17.9
$d_{Fe2}$ (Å)	2.35	2.37 · 2.41 · 2.37	2.35
$\omega_{1(Fe2)}$ (°)	50.2	46.2 · 42.9 · 46.8	49.4
$L_{Fe2}$ (Å)	16.8	18.5 · 20.2 · 18.2	17.1
$d_T$ (Å)	9.56	9.67 · 9.68 · 9.60	9.59
$\omega_{1T}$ (°)	85.3	75.8 · 69.8 · 75.0	81.9
$L_T$ (Å)	40.3	45.9 · 49.9 · 46.1	42.2

<sup>a</sup> The three values correspond to the three crystallographic independent helicates in the crystal lattice.

The structural study of the two symmetric [Fe<sub>2</sub>(LA)<sub>3</sub>] and [Fe<sub>2</sub>(H<sub>2</sub>LB)<sub>3</sub>] metallohelicates evidence that the differences in the external groups of their strands do not significantly alter the supramolecular recognition. Thus, combining both, phenyl and hydroxyphenyl groups in the same ligand could be used to impose asymmetry in the supramolecular architecture without influencing the helicoidal motif or the metallic environment. In order to explore such a possibility, we decided to synthesize the new asymmetric ligand H<sub>3</sub>LC (Scheme 1). This preparation was not trivial. Following various fruitless attempts to use methods analogous to that used for H<sub>2</sub>LA and H<sub>4</sub>LB (Scheme S1), 3-(methoxycarbonyl)-carboxylic acid was treated with one equivalent of acetophenone to obtain the corresponding  $\beta$ -diketone through a Claisen condensation (Scheme 2). The carboxylic group of the resulting molecule was then subject to an esterification with 2-hydroxyacetophenone. The resulting phenoxycarbonyl is then poised to suffer the attack by the enolate from its own acetyl group *via* the so-called Baker-Venkataraman rearrangement (Scheme 2),<sup>22-24</sup> producing H<sub>3</sub>LC as a yellow solid.



**Scheme 2.** Synthesis of asymmetric  $H_3LC$  ligand by combination of Claisen condensation and Baker-Venkataraman rearrangement.

This strategy had been previously used by some of us to make bis- $\beta$ -diketones incorporating hydroxyphenyl groups.<sup>12</sup> The identity of this asymmetric ligand and of all the intermediates was unambiguously confirmed by  $^1\text{H}$  NMR (Figs. S5–S8). The coordination chemistry of  $\text{H}_3\text{LC}$  was then explored through reactions with  $\text{FeCl}_3$  or  $\text{GaCl}_3$  in  $\text{CH}_2\text{Cl}_2$  under basic conditions. The resulting solutions afforded the corresponding asymmetric helicites,  $[\text{Fe}_2(\text{HLC})_3]$  (**3**) and  $[\text{Ga}_2(\text{HLC})_3]$  (**4**), as plate-type crystals after slow diffusion of toluene. Both compounds were isostructural and were best modeled in the non-centrosymmetric  $Cc$  space group (Table S5) although the corresponding centrosymmetric  $C2/c$  and chiral  $C2$  space groups were also explored (see refinement details in Supporting Information). The two helicites are structurally similar to their corresponding symmetric analogues, with two metal ions wrapped by three ligands (Fig. 1, bottom, and Figs S9 and S10), the unit cell constituting a pure racemic mixture of both, the right-handed ( $\Delta\Delta$ ) and the left-handed ( $\Lambda\Lambda$ ) enantiomers. Each metal site features a distorted octahedral environment (analyzed here by CShMs, Table S4) using a  $\beta$ -diketonate unit from each of the three non-equivalent  $\text{HLC}^{2-}$  ligands. The latter are disposed in a head-to-head-to-tail fashion, preferred over the head-to-head-to-head distribution. The two metal centers are separated by 7.21 and 7.20 Å for **3** and **4**, respectively (Tables S6 and S7). As expected, the asymmetric entities preserve similar twisting abilities, as depicted by the values of local and total pitches (Table 1). Interestingly, the values were found to be in between those from  $[\text{Fe}_2(\text{LA})_3]$  and  $[\text{Fe}_2(\text{H}_2\text{LB})_3]$ , in accordance with the hybrid nature of the ligands of these helicites. The stability of the new helicites  $[\text{Ga}_2(\text{H}_2\text{LB})_3]$  (**2**) and  $[\text{Ga}_2(\text{HLC})_3]$  (**4**) in solution was assessed using  $^1\text{H}$  NMR spectroscopy. Complex **2** is soluble in  $\text{CD}_3\text{Cl}$  producing in this solvent a clean spectrum, consistent with the expected idealized symmetry (Fig. 2, top). The latter features nine signals, analogous to these shown by the free ligand<sup>25</sup> (SI) without the peak of the enolic  $-\text{OH}$ . Complex **4** is only scarcely soluble in DMF. In this solvent it produces a more complex spectrum (Fig. 2, bottom) consistent with the lack of mirror symmetry of  $\text{HLC}^{2-}$ .

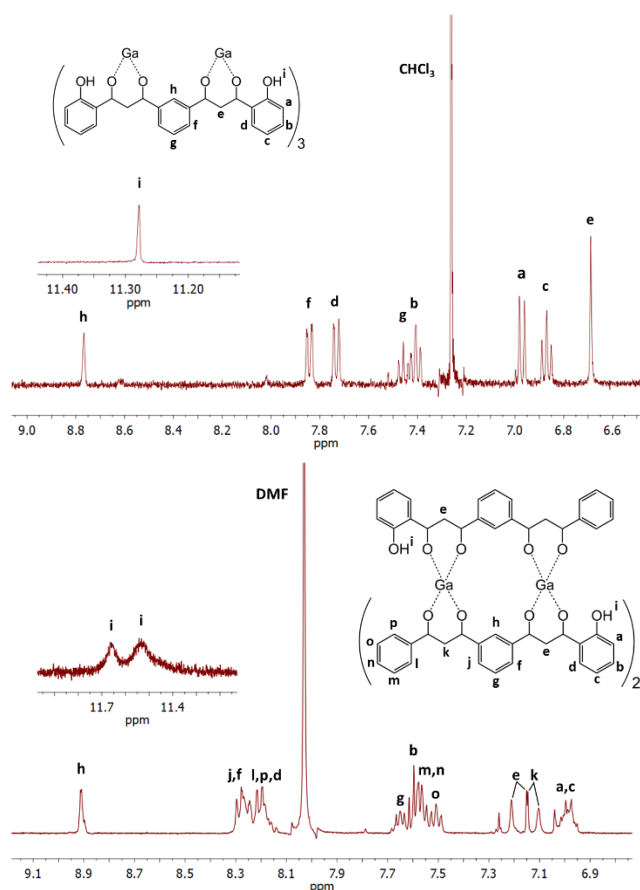


**Figure 2.**  $^1\text{H}$  NMR spectra featuring the aromatic region of  $[\text{Ga}_2(\text{H}_2\text{LB})_3]$  (**2**; top,  $\text{CD}_3\text{Cl}$  as solvent) and  $[\text{Ga}_2(\text{HLC})_3]$  (**4**; bottom,  $d_7$ -DMF as solvent). The inset of the bottom spectrum shows the signals corresponding to the phenol  $-\text{OH}$  groups of compound **4**.

The asymmetry of the complex is only reflected by the splitting of the peaks corresponding to the phenol  $-\text{OH}$  groups (inset Fig. 2, bottom) and the peaks most directly connected to the metals ( $e$  and  $k$  in Fig. 2, bottom). The remainder of

the signals are not sensitive to the configuration of the ligands within the molecule. These results are in full agreement with the structure of **4** observed in the solid state.

## Conclusions

In conclusion, we have shown here the first results of a new synthetic approach to make specific non-symmetric helicates with bis-( $\beta$ -diketonate) ligands. Interestingly, the stability of such supramolecular motifs in solution opens the possibility of evaluating their potential towards biomolecular targets. In that sense, we are now implementing this strategy for the production of new asymmetric ligands featuring both hydrogen donor units and moieties favoring  $\pi$ -stacking interactions, from which the resulting helicates could potentially present the characteristics required to significantly enhance DNA bonding.

GA thanks the Generalitat de Catalunya for the prize ICREA Academia 2018 and QUANTERA for project SUMO (through Spanish PCI2018-093106). The authors acknowledge funding by the Spanish MINECO through CTQ2015-68370-P and PGC2018-098630-B-I00 (GA, LAB, DA, MD, RD, PLI and JG) and MAT2014-53961-R and MAT2017-86826-R (OR), as well as through the Juan de la Cierva program IJCI-2016-29901 (DA). This research used resources of the Advanced Light Source, which is a DOE Office of Science User Facility under contract no. DE-AC02-05CH11231 (SJT).

## Conflicts of interest

There are no conflicts to declare.

## Notes and references

1. J. M. Lehn, A. Rigault, J. Siegel, J. Harrowfield, B. Chevrier and D. Moras, *Proc. Nat. Acad. Sci. U.S.A.*, 1987, **84**, 2565-2569.
2. C. Piguet, G. Bernardinelli and G. Hopfgartner, *Chem. Rev.*, 1997, **97**, 2005-2062.
3. M. Albrecht, *Chem. Rev.*, 2001, **101**, 3457-3498.
4. A. D. Faulkner, R. A. Kaner, Q. M. A. Abdallah, G. Clarkson, D. J. Fox, P. Gurnani, S. E. Howson, R. M. Phillips, D. I. Roper, D. H. Simpson and P. Scott, *Nature Chem.*, 2014, **6**, 797-803.
5. Y. Morita, Y. Yakiyama, S. Nakazawa, T. Murata, T. Ise, D. Hashizume, D. Shiomi, K. Sato, M. Kitagawa, K. Nakasuji and T. Takui, *J. Am. Chem. Soc.*, 2010, **132**, 6944-6946.
6. H. Miyake and H. Tsukube, *Chem. Soc. Rev.*, 2012, **41**, 6977-6991.
7. J.-C. G. Bünzli, *Inter. Focus*, 2013, **3**, 20130032.
8. G. Aromí, P. Gamez and J. Reedijk, *Coord. Chem. Rev.*, 2008, **252**, 964-989.
9. A. J. Brock, J. K. Clegg, F. Li and L. F. Lindoy, *Coord. Chem. Rev.*, 2018, **375**, 106-133.
10. R. F. Brissos, L. Korrodi-Gregório, R. Pérez-Tomás, O. Roubeau and P. Gamez, *Chem. Sq.*, 2018, **2**, 4.
11. M. Raja, R. G. Iyer, C. Gwengo, D. L. Reger, P. J. Pellechia, M. D. Smith and A. E. Pascui, *Organometallics*, 2013, **32**, 95-103.
12. J. Salinas-Uber, M. Estrader, J. Garcia, P. Lloyd-Williams, A. Sadurni, D. Dengler, J. van Slageren, N. F. Chilton, O. Roubeau, S. J. Teat, J. Ribas-Arino and G. Aromi, *Chem., Eur. J.*, 2017, **23**, 13648-13659.
13. T. D. Roberts, M. A. Little, L. J. Kershaw Cook and M. A. Halcrow, *Dalton Trans.*, 2014, **43**, 7577-7588.
14. D. Imbert, M. Cantuel, J.-C. G. Bünzli, G. Bernardinelli and C. Piguet, *J. Am. Chem. Soc.*, 2003, **125**, 15698-15699.
15. D. Aguilà, L. A. Barrios, V. Velasco, O. Roubeau, A. Repollés, P. J. Alonso, J. Sesé, S. J. Teat, F. Luis and G. Aromí, *J. Am. Chem. Soc.*, 2014, **136**, 14215-14222.
16. V. A. Grillo, E. J. Seddon, C. M. Grant, G. Aromí, J. C. Bollinger, K. Folting and G. Christou, *Chem. Commun.*, 1997, 1561-1562.
17. E. C. Sanudo, T. Cauchy, E. Ruiz, R. H. Laye, O. Roubeau, S. J. Teat and G. Aromi, *Inorg. Chem.*, 2007, **46**, 9045-9047.
18. L. A. Barrios, D. Aguilà, S. Méllat, O. Roubeau, S. J. Teat, P. Gamez and G. Aromí, *C. R. Chim.*, 2008, **11**, 1117-1120.
19. L. A. Barrios, D. Aguilà, O. Roubeau, P. Gamez, J. Ribas-Arino, S. J. Teat and G. Aromi, *Chem., Eur. J.*, 2009, **15**, 11235-11243.
20. S. Alvarez, D. Avnir, M. Lluell and M. Pinsky, *New J. Chem.*, 2002, **26**, 996-1009.
21. S. Floquet, M. Borkovec, G. Bernardinelli, A. Pinto, L.-A. Leuthold, G. Hopfgartner, D. Imbert, J.-C. G. Bünzli and C. Piguet, *Chem., Eur. J.*, 2004, **10**, 1091-1105.
22. W. Baker, *J. Chem. Soc.*, 1933, 1381-1389.
23. D. C. Bhalla, H. S. Mahal and K. Venkataraman, *J. Chem. Soc.*, 1935, 868-870.
24. H. S. Mahal and K. Venkataraman, *J. Chem. Soc.*, 1934, 1767-1769.

25. G. Aromí, C. Boldron, P. Gamez, O. Roubeau, H. Kooijman, A. L. Spek, H. Stoeckli-Evans, J. Ribas and J. Reedijk, *Dalton Trans.*, 2004, 3586-3592.